Food Chemistry: X 25 (2025) 102147

Contents lists available at ScienceDirect

Food Chemistry: X

journal homepage: www.sciencedirect.com/journal/food-chemistry-x

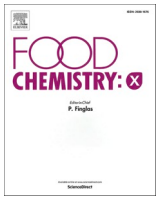

Unraveling the potential of zinc protoporphyrin-forming lactic acid bacteria for replacing nitrite and their role in quality characteristics of Harbin dry sausage

Qianhui Yang, Zhiqiang Feng, Yaru Yuan, Xiufang Xia, Qian Liu, Qian Chen, Baohua Kong *

College of Food Science, Northeast Agricultural University, Harbin, Heilongjiang 150030, China

ARTICLE INFO

Keywords:
Ferrochelatase
Harbin dry sausage
Meat color
Nitrite substitution
Zinc protoporphyrin

ABSTRACT

This study evaluated the effects of zinc protoporphyrin-producing lactic acid bacteria specifically *Weissella viridescens* JX11, *Weissella viridescens* MDJ8, and *Lactobacillus pentosus* Q on nitrite substitution and the quality characteristics of Harbin dry sausage. The redness (a^*) values in the bacteria-inoculated groups were significantly higher than those in the control group ($P < 0.05$) during fermentation. Bacteria-inoculated sausages exhibited a higher proportion of oxymyoglobin and a lower proportion of metmyoglobin ($P < 0.05$). Ferrochelatase activity in the inoculated groups was significantly higher than in the control at days 3 and 6 ($P < 0.05$). Additionally, the fluorescence intensity of zinc protoporphyrin and its precursor, protoporphyrin IX, in the bacteria-inoculated groups significantly increased during fermentation ($P < 0.05$), and *W. viridescen* JX11 exhibited the highest fluorescence intensity and UV–Vis absorption peak ($P < 0.05$). These results suggest that zinc protoporphyrin-producing lactic acid bacteria could potentially replace nitrite in fermented dry sausages.

1. Introduction

Dry sausage, a traditional fermented meat product, is favored by consumers for its unique, chewy texture and distinct fermented flavor. Harbin dry sausage, in particular, is highly popular in northeast China (Hu et al., 2021). The production of dry sausage involves changes in physicochemical properties, enzyme activity, and bacterial counts. Nitrite, a crucial curing agent, plays a significant role in the meat processing industry due to its ability to inhibit spoilage bacteria, provide antioxidative effects, enhance flavor formation, and contribute to the attractive color of the product (Gill & Holley, 2003; Jo, Lee, Yong, Choi, & Jung, 2020). With nitrite, the color of cured meat products will change to a typical red. However, due to the potential health risks associated with nitrite, its use is strictly regulated. Moreover, there is growing consumer demand for nitrite-free meat products as awareness of healthy eating increases. As a result, finding effective alternatives to nitrite remains a major challenge for the meat industry.

Mat color is primarily determined by pigment proteins, with myoglobin (Mb) playing a key role. The different forms and relative concentrations of Mb directly determine the color of meat. The three main forms of Mb are bright red oxymyoglobin (OxyMb), purplish-red deoxymyoglobin (DeoMb), and reddish-brown metmyoglobin (MetMb) (Suman & Joseph, 2013). Mb binds with nitric oxide in cured meat to form nitrosylmyoglobin (NOMb), which imparts a pinkish-red color. The commonly recognized pigment substances in cured meat products are NO-Mb and zinc protoporphyrin (ZnPP), depending on the metal ion at the center of the heme (Yang, Liu, Chen, Li, & Kong, 2023).

ZnPP is a red pigment naturally produced during the fermentation of meat products, where it forms a complex with protoporphyrin IX (PPIX) by coordinating with Zn^{2+} (Al-Murshedi et al., 2025; Wannas, Azooz, Ridha, & Jawad, 2023) and is effective in improving the color of meat products (Wakamatsu, Ito, Nishimura, & Hattori, 2007). ZnPP was first identified in traditional Italian dry-cured ham, and due to its remarkable stability against light and heat, it holds significant potential for application in meat products (Morita, Niu, Sakata, & Nagata, 1996). There are three possible pathways for ZnPP formation: non-enzymatic reactions, enzymatic reactions involving ferrochelatase (FECH) that catalyze the insertion of Zn^{2+} into PPIX, and bacteria-induced enzyme reactions (Wakamatsu, 2022). Although there has been some research on ZnPP formation and characteristics, studies on ZnPP-forming LAB as potential nitrite substitutes in starter cultures are limited. Asaduzzaman, Ohya, Kumura, Hayakawa, and Wakamatsu (2020) evaluated the potential of LAB to replace nitrite in enhancing the color of meat products by examining their ZnPP-forming ability. The results revealed that three

* Corresponding author.
E-mail address: kongbh63@hotmail.com (B. Kong).

https://doi.org/10.1016/j.fochx.2024.102147
Received 15 September 2024; Received in revised form 18 December 2024; Accepted 28 December 2024
Available online 30 December 2024

edible bacteria- *Enterococcus faecium, Leuconostoc mesenteroides*, and *Lactococcus lactis*- exhibited higher ZnPP autofluorescence and produced a brighter red color in salt-added minced meat. Kauser-Ul-Alam, Hayakawa, Kumura, and Wakamatsu (2021) also screened LAB from various sources and identified thirteen LAB strains with strong ZnPP-forming capabilities in minced meat. Wu et al. (2023) isolated *Leuconostoc* strains from spoiled hams and noted their high ZnPP-forming ability.

In a previous study (unpublished data), we screened ZnPP-forming LAB from different sources and identified three strains *Weissella viridescens* JX11, *Weissella viridescens* MDJ8, and *Lactobacillus pentosus* Q that demonstrated superior ZnPP-forming ability. Nitrite can contribute to the attractive color of the product, inhibit spoilage bacteria, enhance flavor formation, and provide antioxidative effects. This study aimed to investigate the potential of these three high ZnPP-forming LAB as a potential substitute for nitrite to improve color and unravel their role on the quality characteristics of Harbin dry sausage by assessing instrumental color, visible images, myoglobin forms, physicochemical properties, microbial counts, and ferrochelatase (FECH) activity. Additionally, changes in ZnPP and PPIX levels in sausage extracts were analyzed using fluorescence and absorption spectroscopy at various fermentation stages.

2. Materials and methods

2.1. Materials and chemicals

Fresh back fat and lean pork were purchased from a local market in Harbin, Heilongjiang, China, within 24 h post-mortem. Adenosine 5′-triphosphate (ATP), ZnPP, and protoporphyrin IX (PPIX) were obtained from Yuanye Bio-Technology Co., Ltd. (Shanghai, China). Acetone, ethanol, zinc chloride ($ZnCl_2$), potassium chloride (KCl), ethylenediaminetetraacetic acid (EDTA), sodium nitrite, tris(hydroxymethyl) aminomethane (Tris), and hydrochloric acid (HCl) were sourced from Solarbio Science & Technology Co., Ltd. (Beijing, China). All reagents used in this experiment were of analytical grade.

2.2. Instrumentals

The ZE-6000 colorimeter, equipped with D65 illuminant, a 50 mm aperture, and a 10° observer angle, was from Nippon Denshoku, Kogyo Co., Ltd. (Tokyo, Japan). The digital camera was from Rongyao Engineering Supervision Co., Ltd. (Henan, China). The multifunctional enzyme marker was from Tecan Trading Co., Ltd. (INFINITE M200 PRO, Shanghai, China). The AquaLab 4 TE DUO was from Decagon Devices, Inc. (Pullman, WA, USA). The TA.XT. Plus Texture Analyser was from Stable Micro Systems Ltd. (Surrey, UK). The digital thermostat water bath was from Instrument Manufacturing Co., Ltd. (HH-4, Rongxing, Changzhou, China). The multifunctional enzyme marker was from Tecan Trading Co., Ltd. (INFINITE M200 PRO, Shanghai, China). The RF6000 fluorescence spectrophotometer was from (Shimadzu Production Co., Ltd. Tokyo, Japan). The UT1810 UV–Vis spectrophotometer was from Purkinje General Instrument, Ltd. (Beijing, China).

2.3. Starter culture preparation

The three LAB strains *W. viridescens* JX11, *W. viridescens* MDJ8, and L. *pentosus* Q- were used as starter cultures, having demonstrated high ZnPP-forming abilities in a previous experiment (unpublished data). Each strain was individually cultured in sterile De Man, Rogosa, and Sharpe (MRS) broth at 37 °C for 16 h and then maintained at 4 °C until use.

2.4. Preparation of Harbin dry sausage

Harbin dry sausages were manufactured following the method of Hu et al. (2021) with slight changes. Fat (600 g) and Lean pork (5400 g) were minced using a 1.5 cm plate and seasoned with the following ingredients (g/kg meat): mixed spices (8.0 g), monosodium glutamate (3.0 g), soft sugar (10.0 g), NaCl (25.0 g), water (50.0 g), and Daqu wine (42 % vol) (10.0 g). Five treatments were applied, including control group, nitrite group (0.1 g/kg), and three bacteria-inoculated groups separately inoculated with *W. viridescens* JX11, *W. viridescens* MDJ8, or L. *pentosus* Q at a concentration of 10^7 CFU/g of meat. The sausages were dried at 25 ± 2 °C for 24 h at a relative humidity of 30 % to 50 %, then transferred to a controlled environment chamber for fermentation at 25 ± 2 °C and 65 % to 75 % relative humidity. Instrumental color, visible images, and physicochemical properties of the sausage samples were evaluated on days 0, 3, 6, and 9 of fermentation.

2.5. Instrumental color and visible images

The instrumental color was measured using a ZE-6000 colorimeter. The results were reported as a^* (redness) and b^* (yellowness) values. Visual images of the samples were captured using a digital camera.

2.6. Determination of the existing forms of Mb

The existing forms of Mb in the dry sausages were determined following the method described by Zajac, Zajac, and Dybas (2022), with slight modifications. Briefly, 5 g of the sample was mixed with 25 mL of 40 mM cold phosphate buffer (pH 6.8). The absorbance values of the resulting supernatant were measured using 96 microplates with a multifunctional enzyme marker at 572, 565, 545, and 525 nm. The proportions of the three Mb forms were calculated as follows:

$$\text{MetMb}\ [\%] = (1.098 + 0.800 \times R_1 + 0.777 \times R_2 - 2.514 \times R_3) \times 100 \quad (1)$$

$$\text{OxyMb}\ [\%] = (-0.361 + 0.809 \times R_1 - 1.267 \times R_2 + 0.882 \times R_3) \times 100 \quad (2)$$

$$\text{DeoMb}\ [\%] = (0.015 - 0.941 \times R_1 + 1.140 \times R_2 + 0.369 \times R_3) \times 100 \quad (3)$$

Where:

$R_1 = A_{545}/A_{525}$, $R_2 = A_{565}/A_{525}$, $R_3 = A_{572}/A_{525}$.

A_{525}, A_{545}, A_{565}, and A_{572} correspond to the absorbance values at 525, 545, 565, and 572 nm, respectively.

2.7. Physicochemical characteristics

The moisture content of the dry sausage was determined following the method of Hu et al. (2021). Water activity (a_w) was determined at room temperature using the AquaLab 4 TE DUO. The pH was determined with an FE20 pH meter according to the method described by Chen et al. (2021). The pH meter was calibrated before use with standard solutions provided by the manufacturer (pH 4 and 7). For shear force determination, dry sausage samples were steamed at 100 °C for 15 min, cooled to room temperature, and then tested using a TA.XT. Plus Texture Analyser, as described by Hu et al. (2021).

2.8. Microbial counts

The total viable counts and LAB counts were determined following the method of Mikami et al. (2020). Briefly, a 10 g sausage sample was diluted with 90 mL of sterile saline, homogenized, and serially diluted. Each dilution (1 mL) was plated in triplicate on plate count agar and MRS agar. After incubating at 37 °C for 48 h, counts were determined.

2.9. Ferrochelatase activity determination

FECH activity was assessed based on the fluorescence intensity of ZnPP formation, as described by Parolari, Benedini, and Toscani (2009), with slight modifications. Briefly, a 5 g sample was homogenized for 2

min with 30 mL of ice-cold extraction buffer. The homogenate was ultrasonicated for 15 min at 450 W, followed by centrifugation at 15,000 ×*g* for 5 min. The supernatant was used for subsequent enzyme assays.

Each supernatant (100 μL) was mixed with 50 μL of 800 μM $ZnCl_2$, followed by the addition of 40 μL of 25 mM ATP. Finally, 10 μL of 1 mM protoporphyrin IX was added. A blank was prepared by adding 70 μL of 50 mM EDTA to the reaction mixture. The mixture was incubated in darkness at 37 °C for 45 min in a digital thermostat water bath. After incubation,70 μL of EDTA was added to stop the enzymatic reactions, and the tubes were placed in an ice-cold bath for 5 s. FECH activity was then determined using a multifunctional enzyme marker. A standard curve equation was used to quantify ZnPP concentrations within the range of 0.319 to 0.958 μM. The standard curve equation ($R^2 = 0.9990$) is shown as:

$$C_{ZnPP}\ (nm/mL) = \frac{F - 464.67}{53891} \quad (4)$$

where C_{ZnPP} is the concentration of ZnPP (nm/mL), and *F* is the fluorescence intensity in the extracts catalyzed by FECH. One FECH activity unit is defined as the amount of enzyme per gram of sample that catalyzes 1 nmol product ZnPP per hour.

2.10. Fluorescence and UV–vis spectroscopy analysis of sausage extracts

PPIX and ZnPP were extracted as detailed by Wakamatsu, Ito, et al. (2007) with minor modifications. Minced sausage samples (4 g) were added to 20 mL of 75 % acetone. After stirring, the sample tubes were kept at 4 °C in the dark for 30 min, then centrifuged at 10,619 ×*g* for 5 min at 4 °C. The final supernatant was analyzed by the RF6000 fluorescence spectrophotometer. PPIX in the sausage extracts was measured at 610 to 660 nm with excitation at 410 nm, and the fluorescence peak at 632 nm indicated PPIX. Similarly, ZnPP was measured at 540 to 660 nm with excitation at 420 nm, and the fluorescence peak at 590 nm indicated ZnPP. All extraction operations were performed in the dark to minimize ZnPP degradation. The extracts were also analyzed using absorption spectroscopy, with spectra recorded from 400 to 600 nm on a UT1810 UV–Vis spectrophotometer.

2.11. Statistical analysis

The experimental data were presented in terms of mean values ± standard error (SE) and were subjected to statistical analysis employing SPSS Statistics 22.0 software (SPSS Inc., IL, USA). A one-way ANOVA complemented by Duncan's multiple range test was utilized to evaluate statistical significance at $P < 0.05$. All experimental procedures involving sausage samples were carried out in triplicate, with each trial independently replicated three times to ensure reliability. Graphs were prepared using Origin Pro 2021 (Origin Lab Co., Northampton, MA, USA).

3. Results and discussion

3.1. Color analysis and visible images

The effect of ZnPP-forming bacteria on the instrumental color and visible images of dry sausages is presented in Fig. 1. The *a** values of dry sausages decreased with fermentation time in all groups except the nitrite group. In the nitrite group, the *a** values initially increased and then decreased, likely due to the oxidation of Mb to MetMb, and the subsequent reduction of MetMb to NOMb (Gøtterup et al., 2008; Hayes, Canonico, & Allen, 2013). The *a**-value of bacteria-inoculated groups was significantly higher than that of the control group after 3-day of fermentation ($P < 0.05$), especially *W. viridescens* JX11 and *W. viridescens* MDJ8 groups. At the termination of fermentation, no significant discrepancy was observed in the *a** values between the *W. viridescens* JX11 group and the nitrite group ($P > 0.05$). The bright red color in the nitrite group was primarily attributed to NOMb production, whereas the red color in the bacteria-inoculated groups was likely due to the formation of ZnPP. Wakamatsu, Nishimura, and Hattori

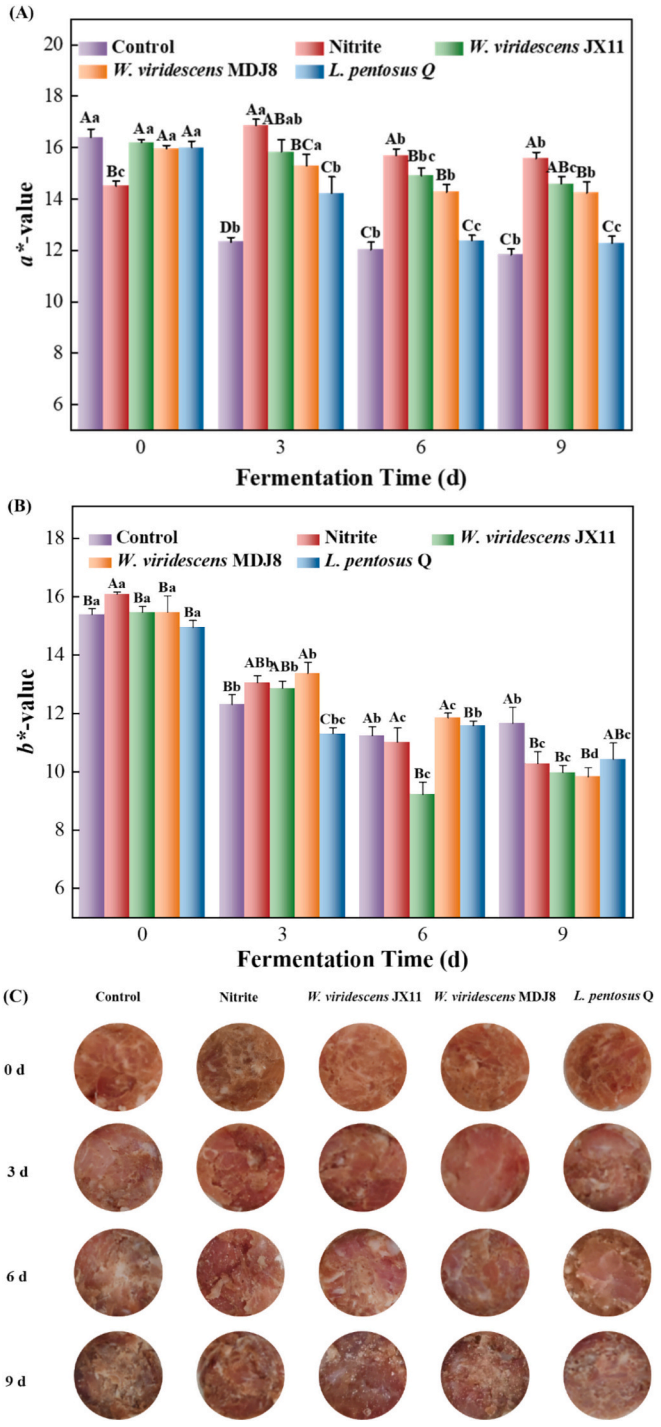

Fig. 1. Impact of three strains of ZnPP-forming LAB on the instrumental color and visual appearance of dry sausage during fermentation. Panels A, B, and C represent the *a** value, *b** value, and visual images of the dry sausage, respectively. The data are presented as mean values ± standard error (SE). Distinct uppercase letters (A–D) denote significant differences between different groups at the same fermentation time, while lowercase letters (a–d) highlight significant differences across fermentation times within the same treatment group ($n = 3$) ($P < 0.05$).

(2004) demonstrated that the formation of ZnPP in Parma ham contributes to the bright red color. As shown in Fig. 1B, there was no significant difference in b^*-values between the bacteria-inoculated and nitrite groups at the end of fermentation ($P > 0.05$). The b^* of the control group was significantly higher than that of the other groups ($P < 0.05$), indicating a visually duller color.

The color of the visual images corresponded with the a^* values (Fig. 1C). At the beginning of fermentation, there were no noticeable visual differences between the control and the bacteria-inoculated groups. The visual color of the nitrite group appeared darker than that of the other groups; however, as fermentation progressed, it became light red. After 3 d of fermentation, the control group displayed a visually duller color than the other groups, likely due to the formation of MetMb (Ning et al., 2019). The visual appearance of the bacteria-inoculated groups was close to that of the nitrite group, especially *W. viridescens* JX11 and *W. viridescens* MDJ8 groups, having a cherry-red color, indicating that the ZnPP-forming bacteria have the potential to produce an acceptable red hue.

3.2. Forms of Mb

MetMb, OxyMb, and DeoMb are the three forms of Mb, and their percentage changes in dry sausage throughout the fermentation period are shown in Fig. 2. At day 0, the relative content of MetMb in the nitrite group was significantly higher and the relative content of OxyMb was significantly lower than in the other groups ($P < 0.05$). Mb (Fe^{2+}) is easily oxidized to MetMb in the early stages of meat fermentation due to the effect of nitrite on Mb (Jo et al., 2020), leading to a gray color in meat products, consistent with the a^* and visual images of the nitrite group in Figs. 1A and C. As fermentation progressed, the MetMb percentage in the nitrite group initially decreased and then increased. In the control and bacteria-inoculated groups, the MetMb percentage gradually increased, while the OxyMb percentage gradually decreased. During fermentation, DeoMb and OxyMb levels were not highly stable and easily transferred into brownish MetMb. After 9 d of fermentation, the OxyMb percentage in the bacteria-inoculated groups was significantly higher, and the MetMb percentage was significantly lower than in the control and nitrite groups ($P < 0.05$), particularly in the *W. viridescens* JX11 and *W. viridescens* MDJ8 groups, implying that the bacteria-inoculated groups played a role in reducing color oxidation to some extent (Liu, Liu, Jiang, Yan, & Qi, 2015).

3.3. Physicochemical analysis

The moisture content and water activity of all groups significantly decreased during fermentation ($P < 0.05$), as shown in Figs. 3 A and B. Similar results were reported by Hu et al. (2021). At the start of the fermentation (0 d), the initial moisture content and water activity were

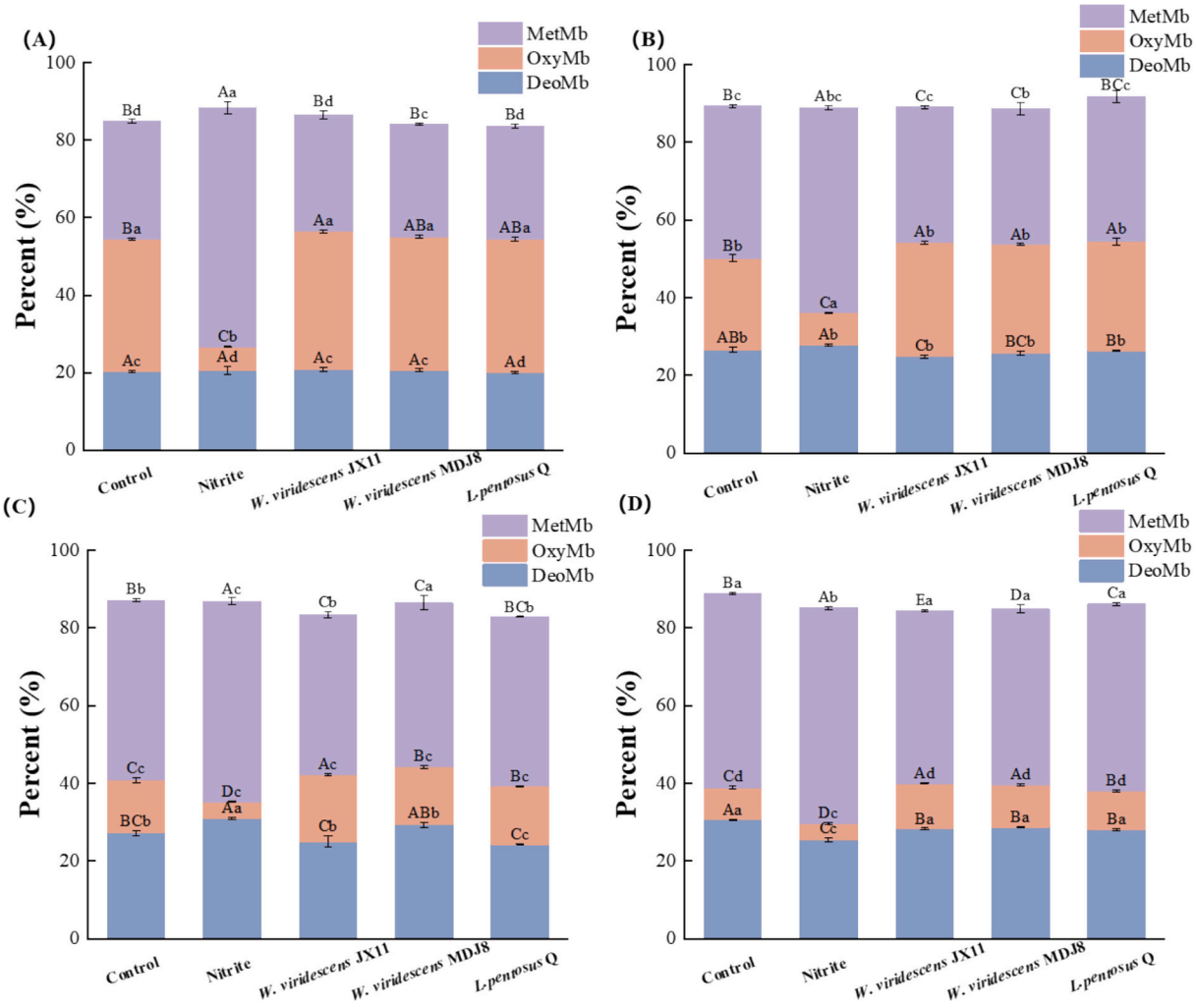

Fig. 2. Variation in the percentage of Mb forms in dry sausage during fermentation. Panels A, B, C, and D correspond to fermentation durations of 0, 3, 6, and 9 d, respectively. Data are presented as mean values ± standard error (SE). Distinct uppercase letters (A–E) indicate significant differences between different groups at the same fermentation time, while lowercase letters (a–d) denote significant differences across fermentation times within the same treatment group (n = 3) ($P < 0.05$).

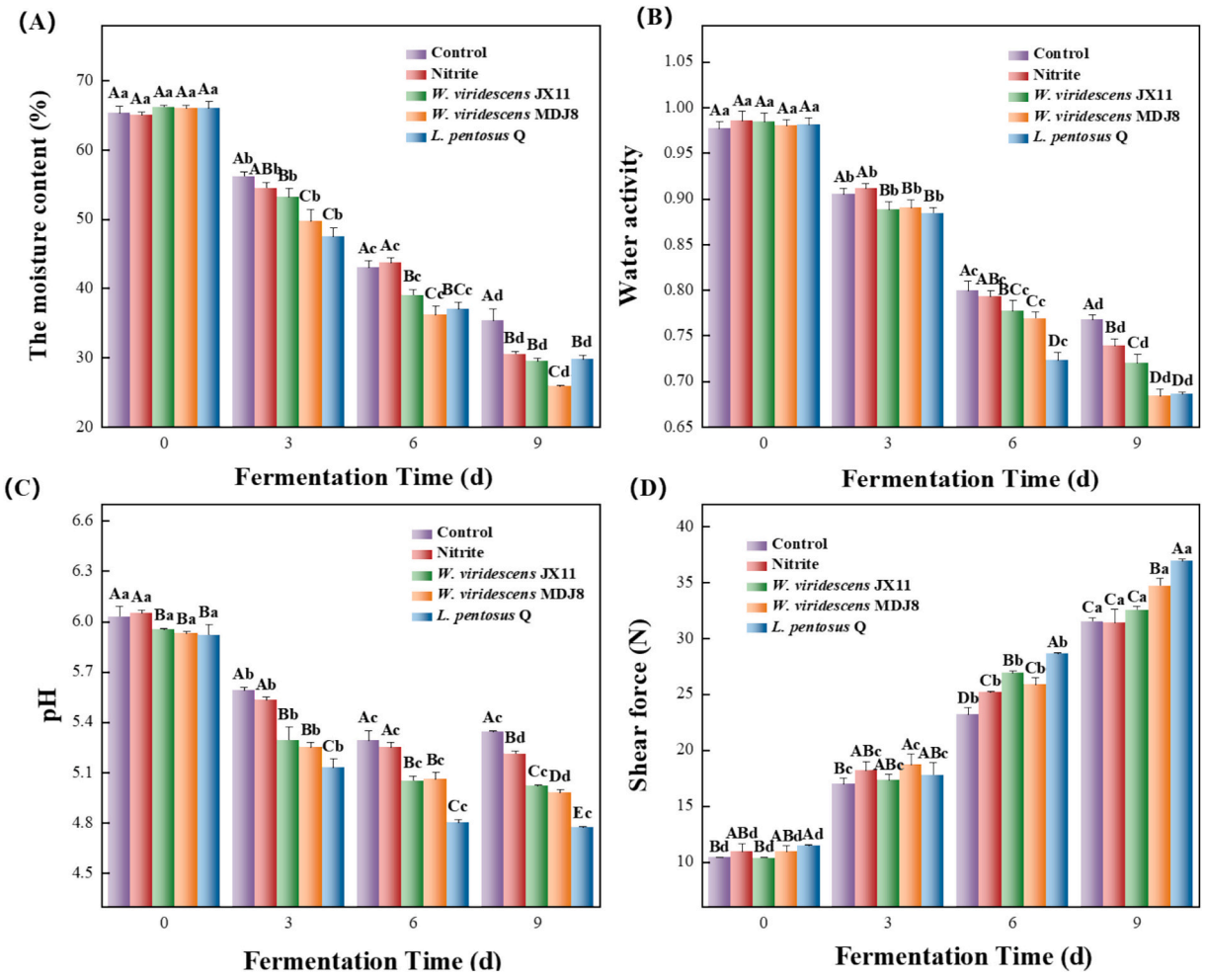

Fig. 3. Evolution of moisture content (A), water activity (B), pH (C), and shear force (D) in dry sausage during fermentation. Data were presented as mean values ± standard error (SE). Different uppercase letters (A–E) signify significant differences between groups at the same fermentation time, while lowercase letters (a–d) indicate significant differences across fermentation times within the same treatment group (n = 3) ($P < 0.05$).

approximately 65.69 % and 0.981, respectively across all groups. After 9 d of fermentation, the moisture content decreased to 35.33 %, 30.50 %, 29.50 %, 25.83 %, and 29.83 % for the control, nitrite, *W. viridescens* JX11, *W. viridescens* MDJ8, and L. *pentosus* Q-inoculated groups, respectively. Correspondingly, water activity decreased to 0.767, 0.739, 0.720, 0.684, and 0.686 ($P < 0.05$). The bacteria-inoculated sausages exhibited lower moisture content and water activity than the control and nitrite groups ($P < 0.05$), attributable to microbial metabolism, and a concurrent decrease in pH (Cavalheiro, Ruiz-Capillas, Herrero, & Pintado, 2021).

The pH of dry sausage in all groups decreased during fermentation (Fig. 3C). Initially, the control and nitrite groups had a pH of approximately 6.04, while the bacteria-inoculated groups had a pH of about 5.93. After 9 d, pH values significantly decreased to 5.34, 5.21, 5.02, 4.98, and 4.77 for the control, nitrite, *W. viridescens* JX11, *W. viridescens* MDJ8, and L. *pentosus* Q-inoculated groups, respectively ($P < 0.05$). The faster pH decline in the bacteria-inoculated groups is attributed to the metabolism of carbohydrates by LAB producing organic acids like lactic and acetic acids, which lower the pH of the dry sausage (Zhao et al., 2011). The L. *pentosus* Q group exhibited a significantly lower pH than the other groups ($P < 0.05$), indicating that L. *pentosus* Q has a stronger acid production capacity, which is beneficial for meat products as the low pH effectively inhibits pathogenic and spoilage microorganisms (Essid & Hassouna, 2013).

The shear force of dry sausage, which reflects the tenderness of the meat product, exhibited an increasing trend across all groups during fermentation (Fig. 3D). Initially, all samples had a shear force of approximately 10.8 N at day 0. After 9 d of fermentation, the shear force significantly increased to 31.49, 31.36, 32.56, 34.71, and 36.90 N for the control, nitrite, *W. viridescens* JX11, *W. viridescens* MDJ8, and L. *pentosus* Q groups, respectively ($P < 0.05$). This increase in shear force correlates with the reduction in internal water content and water activity (Visessanguan et al., 2006).

3.4. Microbial analysis

The total viable counts and LAB counts in all groups exhibited an initial increase followed by a decrease during fermentation (Figs. 4 A and B). The initial load of three bacteria-inoculated groups separately was at a concentration of 10^7 CFU/g of meat. At 0 days, LAB counts were 5.70, 5.67, 6.30, 6.31, and 6.36 log CFU/ g in the control, nitrite, *W. viridescens* JX11, *W. viridescens* MDJ8, and *L. pentosus* Q groups respectively. The initial increase ($P < 0.05$) is due to the high moisture content and rich carbohydrates, which provided a favorable environment for microbial growth. The bacteria-inoculated groups had significantly higher microbial counts than the control and nitrite groups due to the addition of LAB ($P < 0.05$). However, after 3 d of fermentation, the growth rate of total viable counts and LAB counts reduced, likely due to nutrient depletion and the saturation of bacterial growth. By day 9, microbial counts decreased across all groups, which may be attributed to nutrient limitation, the accumulation of metabolites, and reduced water content (Guo et al., 2024; Hu et al., 2020), all of which inhibit microbial

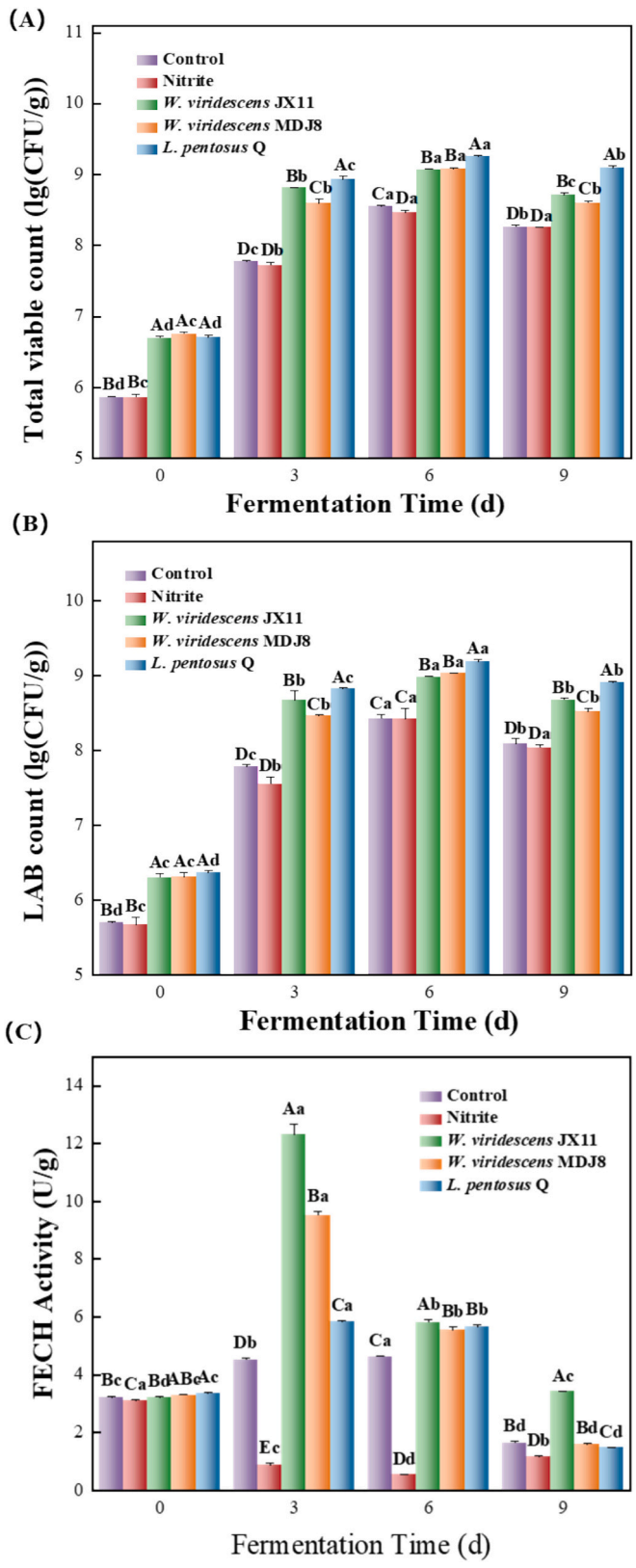

Fig. 4. Changes in total viable count (A), LAB count (B), and FECH activity (C) in dry sausage during fermentation. Data are presented as mean values ± standard error (SE). Distinct uppercase letters (A–D) represent significant differences between different groups at the same fermentation time, while lowercase letters (a–d) denote significant differences across fermentation times within the same treatment group ($P < 0.05$).

activity.

3.5. Ferrochelatase activity analysis

ZnPP is believed to be produced by FECH (Chau, Ishigaki, Kataoka, & Taketani, 2010), a terminal enzyme in the heme biosynthesis pathway in vivo that catalyzes the insertion of Fe^{2+} into PPIX to form heme. Under certain conditions, FECH can also catalyze the insertion of Zn^{2+} into PPIX to produce ZnPP (Chau et al., 2010; Dailey et al., 2000; Taketani et al., 2007). The FECH activity in dry sausages was measured to assess its effect on ZnPP formation during different fermentation periods (Fig. 4C). The enzyme activity in the nitrite group was significantly lower than in the other groups during the fermentation process ($P < 0.05$), likely due to nitrite's inhibitory effect on FECH (Benedini, Raja, & Parolari, 2008). During fermentation, the enzyme activities of all groups, except for the nitrite group, initially increased and then decreased. At 3 and 6 d of fermentation, the bacteria-inoculated groups exhibited significantly higher FECH activity than the control group ($P < 0.05$). Among the bacteria-inoculated groups, the FECH activity in the *W. viridescens* JX11 group was significantly higher than that in the *W. viridescens* MDJ8 and L. *pentosus* Q groups ($P < 0.05$), particularly at day 3. The enzyme activity in all groups markedly decreased by the end of fermentation, indicating that enzymatic reactions predominated in the initial fermentation period of dry sausages, followed by non-enzymatic reactions in the later stages.

3.6. Spectrum analysis of sausage extracts

3.6.1. Fluorescence spectrum analysis of PPIX

PPIX, widely considered a heme precursor, has been extensively studied (Wakamatsu, Okui, Hayashi, Nishimura, & Hattori, 2007). ZnPP formation is closely associated with PPIX, which exhibits a strong fluorescence peak at the excitation of 410 nm and emission of 632 nm (De Maere et al., 2016). Numerous hypotheses have been proposed regarding the formation of ZnPP. Based on the above, we periodically analyzed the fluorescence intensity of PPIX and ZnPP to investigate the mechanism of ZnPP formation.

Based on the fluorescence spectra shown in Figs. 5A-D, no fluorescence peak for PPIX was observed in any group on day 0 of fermentation. As fermentation progressed, the characteristic peaks of PPIX gradually increased in all groups, with a significant rise in the bacteria-inoculated group than that of the control and nitrite groups ($P < 0.05$), especially in the *W. viridescens* JX11 group. The inserted table (Fig. 5 E) shows a significant increase in PPIX fluorescence intensity at 632 nm during the fermentation ($P < 0.05$), except for the nitrite group, where the PPIX peak remained negligible. At the end of fermentation, the *W. viridescens* JX11 group exhibited the highest fluorescence intensity of PPIX, followed by followed by *W. viridescens* MDJ8, *L. pentosus* Q, the control, and the nitrite group.

The nitrite group exhibited almost no specific peaks for PPIX throughout the fermentation, indicating that nitrite inhibits PPIX formation (Wakamatsu, Hayashi, Nishimura, & Hattori, 2010). Initially, no PPIX fluorescence peak was present in any group on day 0, but PPIX fluorescence intensity significantly increased with fermentation time, especially in the bacterial inoculated groups. This increase may be attributed to the decomposition of proteins like Mb and the activity of microorganisms (Grossi, do Nascimento, Cardoso, & Skibsted, 2014; Wakamatsu, Okui, Ikeda, Nishimura, & Hattori, 2004), which promotes the formation of PPIX and ZnPP in dry sausage.

3.6.2. The fluorescence spectrum analysis of ZnPP

ZnPP is a distinct red fluorescent substance with strong fluorescence intensity when excited at 420 nm and emitting at 590 nm (Adamsen, Moller, Laursen, Olsen, & Skibsted, 2006). It is distinguishable from NOMb, which lacks fluorescence. As shown in the fluorescence spectra in Figs. 6A-D, the trend of ZnPP formation across all groups mirrors that

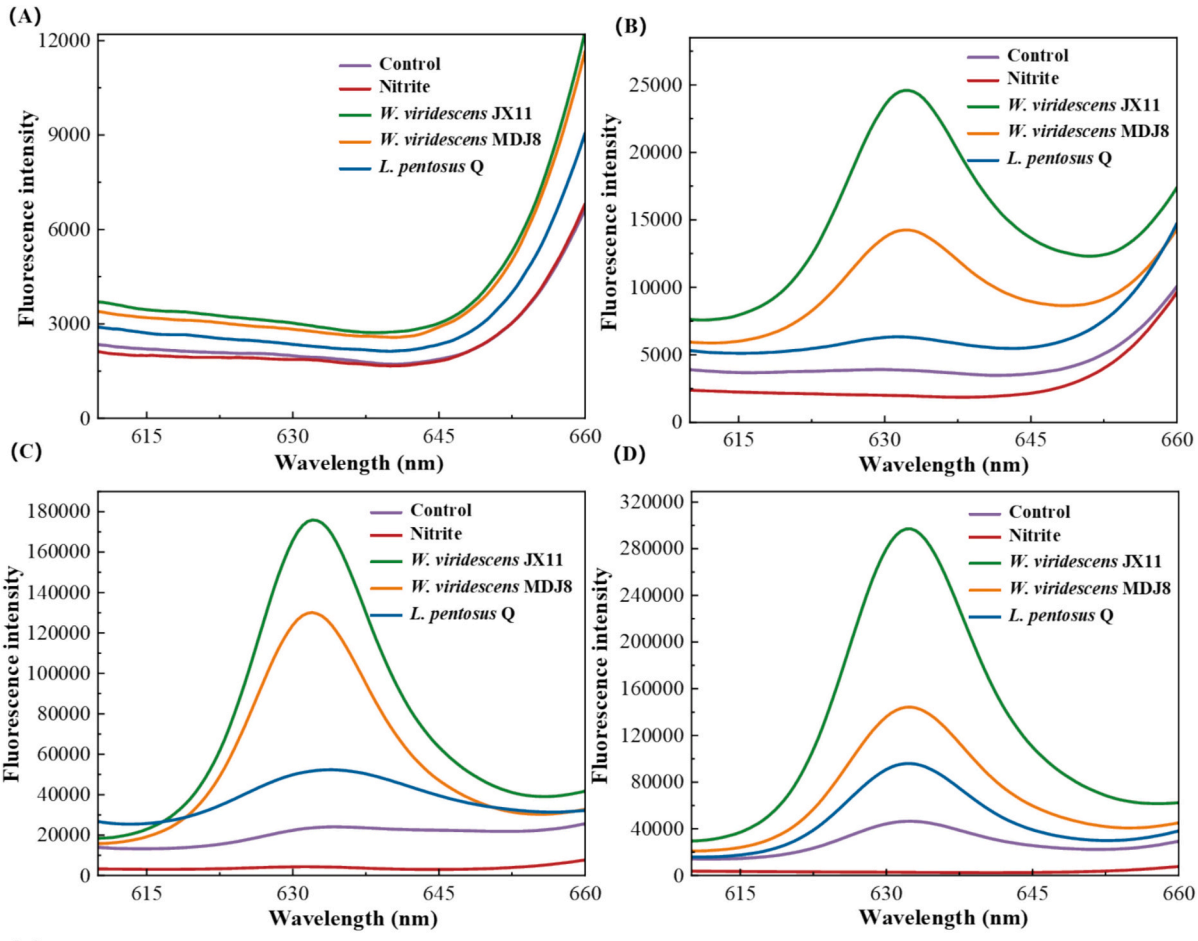

(E)

Sampies	Fermentation Time (d)			
	0	3	6	9
Control	1943 ± 2^{Dd}	3871 ± 2^{Dc}	23529 ± 53^{Db}	46167 ± 196^{Da}
Nitrite	1841 ± 7^{Ed}	1968 ± 13^{Ec}	4312 ± 13^{Ea}	2731 ± 1^{Eb}
W. viridescens JX11	2929 ± 5^{Ad}	24425 ± 121^{Ac}	174176 ± 1238^{Ab}	294591 ± 1660^{Aa}
W. viridescens MDJ8	2757 ± 4^{Bd}	14163 ± 63^{Bc}	128827 ± 889^{Bb}	143099 ± 762^{Ba}
L. pentosus Q	2291 ± 1^{Cd}	6311 ± 10^{Cc}	51701 ± 40^{Cb}	95263 ± 503^{Ca}

Fig. 5. Changes in the fluorescence spectrum of PPIX extracts in dry sausage during fermentation. Panels A, B, C, and D correspond to fermentation periods of 0, 3, 6, and 9 d, respectively. Panel E is an inset table of the fluorescence intensity analysis ($E_x = 410$ nm, $E_m = 632$ nm). Data are expressed as mean values ± standard error (SE). Different uppercase letters (A–E) indicate significant differences between treatment groups at the same fermentation time, while different lowercase letters (a–d) signify significant differences across fermentation times within the same treatment group (n = 3) ($P < 0.05$).

of PPIX formation in Fig. 5. At day 0, all groups exhibited very low fluorescence peaks of ZnPP. During fermentation, the fluorescence peak significantly increased in all groups ($P < 0.05$), except for the nitrite group, aligning with previous findings that nitrite can suppress ZnPP formation to some extent (Wakamatsu et al., 2010).

The ZnPP content in sausage extracts was evaluated by peak intensity. As shown in the inserted table (Fig. 6E), all groups exhibited a significant increase in fluorescence intensity ($P < 0.05$), particularly in the bacteria-inoculated groups. By day 9, the *W. viridescens* JX11 group had the highest fluorescence intensity, followed by *W. viridescens* MDJ8, *L. pentosus* Q, the control, and the nitrite groups, with fluorescence intensities of 343,563, 314,202, 115,670, 127,787, and 13,305, respectively ($P < 0.05$). The increase in fluorescence intensity in the control group may be attributed to the action of endogenous meat enzymes such as FECH, and endogenous microorganisms (Ghadiri Khozroughi, Kroh, Schluter, & Rawel, 2018). The relatively low fluorescence peak in the L. *pentosus Q* group may be attributed to excessively low pH, which is unfavorable for ZnPP formation (de Maere et al., 2016). During fermentation, the activity of FECH in dry sausage initially increased and then decreased (Fig. C), whereas the fluorescence intensity of PPIX and ZnPP consistently increased. This suggests that ZnPP formation in dry sausage is primarily driven by enzymatic reactions in the early fermentation stage, shifting to non-enzymatic reactions in the later stage as bacterial counts and FECH activity decline.

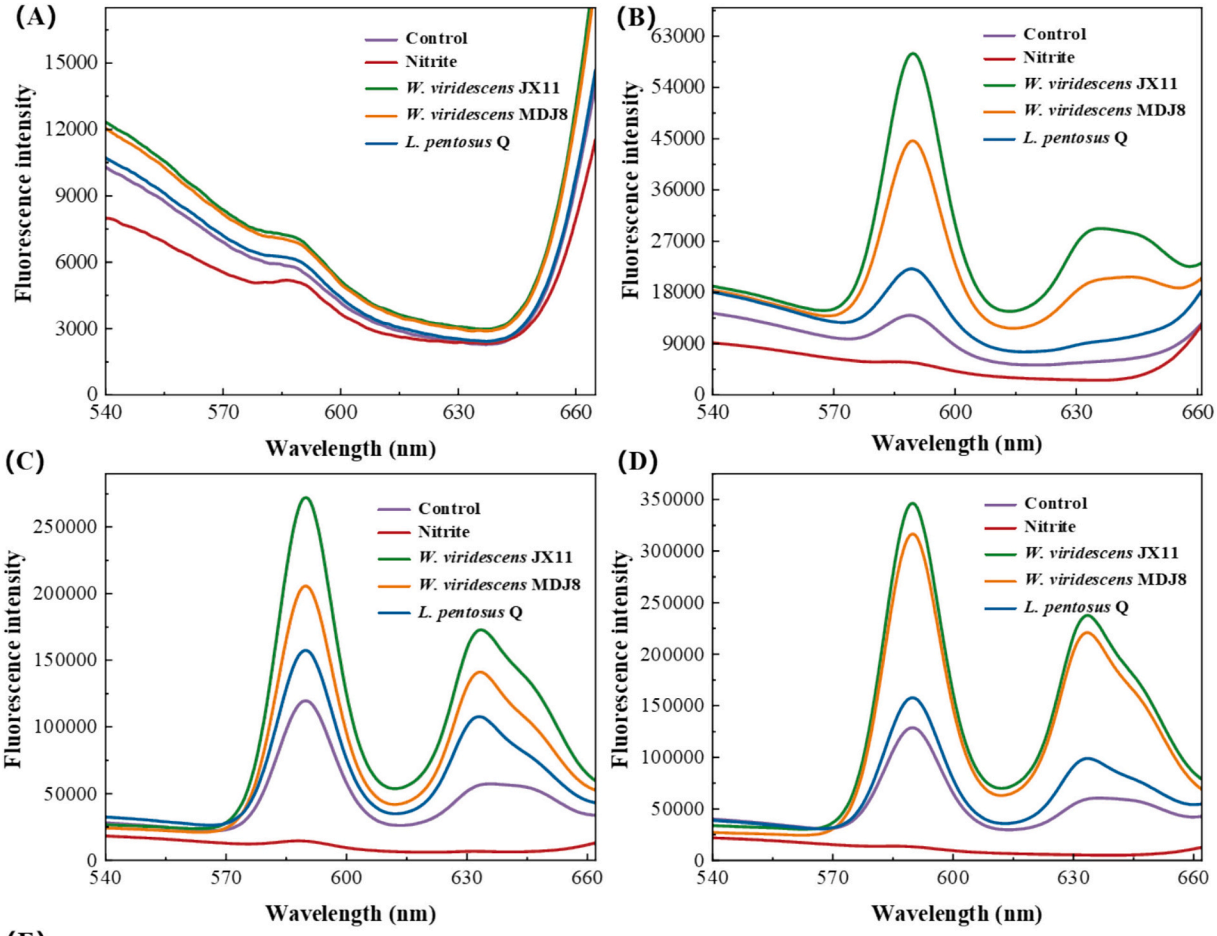

(E)

Sampies	Fermentation Time (d)			
	0	3	6	9
Control	5583 ± 14^{Dd}	13867 ± 12^{Dc}	118834 ± 438^{Db}	127787 ± 463^{Da}
Nitrite	5025 ± 16^{Ed}	5642 ± 3^{Ec}	14240 ± 26^{Eb}	13305 ± 15^{Ea}
W. viridescens JX11	6935 ± 20^{Ad}	59740 ± 90^{Ac}	270139 ± 1100^{Ab}	343563 ± 1438^{Aa}
W. viridescens MDJ8	6749 ± 21^{Bd}	44416 ± 71^{Bc}	204295 ± 789^{Bb}	314202 ± 1259^{Ba}
L. pentosus Q	5969 ± 18^{Cc}	22037 ± 24^{Cb}	156366 ± 565^{Ca}	156707 ± 562^{Ca}

Fig. 6. Changes in the fluorescence spectrum of ZnPP extracts in dry sausage during fermentation. Panels A, B, C, and D present fermentation periods of 0, 3, 6, and 9 d, respectively. Panel E includes an inset table showing the fluorescence intensity analysis (E_x = 420 nm, E_m = 590 nm). Data are expressed as mean values ± standard error (SE). Different uppercase letters (A–E) indicate significant differences between treatment groups at the same fermentation time, while lowercase letters (a–d) denote significant differences across fermentation times within the same treatment group (n = 3) ($P < 0.05$).

3.6.3. *UV–vis spectra analysis*

In addition to fluorescence measurements, spectrophotometric data are valuable for understanding the chemical properties of pigments and reflect the form of Mb derivatives in the extract to some extent. The absorption spectra of extracts from dry sausage during fermentation are shown in Figs. 7A-D, displaying a trend similar to the fluorescence spectra of ZnPP in Figs. 6A-D. As shown in Figs. 7A and B, the UV absorption peak at 417 nm, which is the specific absorption peak of ZnPP, was negligible in all groups on days 0 and 3 of fermentation. However, with the increased fermentation time, the specific absorption peaks of ZnPP increased significantly in all groups ($P < 0.05$).

A higher absorption peak correlates with a stronger fluorescence intensity of ZnPP. The data in the inserted table (Fig. 7E) indicate that the UV–Vis absorbance of the bacteria-inoculated groups was significantly more intense than that of the control group ($P < 0.05$). Notably, the absorption in the *W. viridescens* JX11 group at 9 d of fermentation had the highest absorbance ($P < 0.05$), consistent with the fluorescence intensity results (Fig. 6E). The absence of a specific ZnPP peak in the nitrite group contrasted with the higher specific peaks in the bacteria-inoculated groups, suggests that the red color of the nitrite group is primarily due to NOMb formation, whereas the red color in the bacteria-inoculated groups is likely attributed to ZnPP formation (Gündoğdu, Karahan, & Çakmakç, 2006; Wakamatsu, Nishimura, & Hattori, 2004). The absorption of ZnPP in the bacteria-inoculated groups was significantly higher than that of the control group and the nitrite group ($P < 0.05$), indicating that nitrite addition inhibits ZnPP formation, whereas

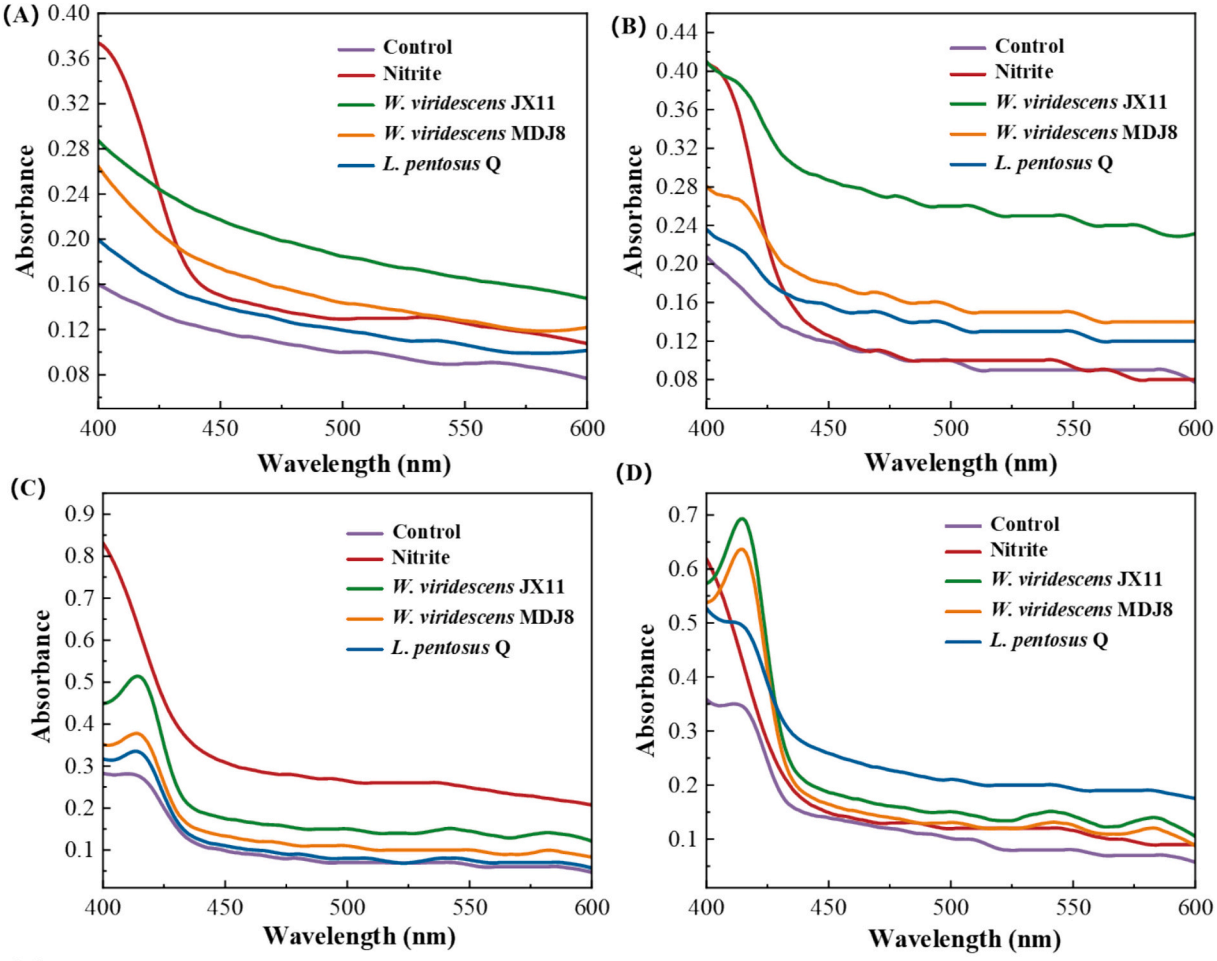

(E)

Sampies	Fermentation Time (d)			
	0	3	6	9
Control	1414 ± 3^{Dd}	1676 ± 4^{Dc}	2660 ± 6^{Db}	3335 ± 10^{Da}
W. viridescens JX11	2562 ± 3^{Ad}	3727 ± 18^{Ac}	4978 ± 23^{Ab}	6727 ± 35^{Aa}
W. viridescens MDJ8	2210 ± 5^{Bd}	2551 ± 22^{Bc}	3636 ± 14^{Bb}	6160 ± 32^{Ba}
L. pentosus Q	1719 ± 2^{Cd}	2057 ± 12^{Cc}	3220 ± 13^{Cb}	4817 ± 12^{Ca}

Fig. 7. Changes in the UV–Vis absorption spectra of ZnPP extracts in dry sausage during fermentation. Panels A, B, C, and D correspond to fermentation periods of 0, 3, 6, and 9 d, respectively. Panel E is an inset table of the absorption intensity at 417 nm (Abs$\times 10^{-4}$). Data are expressed as mean values ± standard error (SE). Different uppercase letters (A–D) indicate significant differences between treatment groups at the same fermentation time, while different lowercase letters (a–d) signify significant differences across fermentation times within the same treatment group (n = 3) ($P < 0.05$).

bacterial inoculation greatly enhances ZnPP formation, thereby improving the color of dry sausages.

4. Conclusions

The potential of ZnPP-forming LAB strains (*W. viridescens* JX11, *W. viridescens* MDJ8, and L. *pentosus* Q) to replace nitrite in Harbin dry sausage was evaluated. The a^* and visible color in *W. viridescen* JX11 and *W. viridescen* MDJ8 groups surpassed those of the control group, showing color profiles similar to the nitrite-treated group. The LAB-inoculated groups also exhibited elevated FECH activities. Based on FECH activity, fluorescence intensity, and UV–Vis analysis, it is suggested that ZnPP formation in dry sausage occurs predominantly via FECH reactions in the early fermentation stages and non-enzymatic processes later on. Overall, the results demonstrated that *W. viridescen* JX11 had the best potential as a nitrite substitute and may be a more suitable strain to improve the color of dry fermented products. The findings from this study may provide the meat industry the safer and more effective ZnPP-forming strains which has the potential to replace nitrite to improve the color of meat products and satisfy consumer demand for healthy meat products. In the further studies, the effect of these ZnPP-forming LAB on other properties of fermented meat products, such as sensory attributes, flavor, and antioxidant capacity need to be evaluated, and the impact of different fermentation conditions and different ZnPP-forming LAB combination also need to be investigated.

CRediT authorship contribution statement

Qianhui Yang: Writing – original draft, Methodology. **Zhiqiang Feng:** Validation, Software, Investigation. **Yaru Yuan:** Data curation. **Xiufang Xia:** Visualization, Data curation. **Qian Liu:** Software, Investigation. **Qian Chen:** Visualization, Resources. **Baohua Kong:** Writing – review & editing, Supervision, Funding acquisition, Conceptualization.

Declaration of competing interest

The authors declare that they have no known competing financial interests or personal relationships that could have appeared to influence the work reported in this paper.

Acknowledgments

This study was funded by the National Natural Science Foundation in China (32372373 and U22A20547).

Data availability

Data will be made available on request.

References

Adamsen, C. E., Moller, J. K., Laursen, K., Olsen, K., & Skibsted, L. H. (2006). Zn-porphyrin formation in cured meat products: Effect of added salt and nitrite. *Meat Science, 72*(4), 672–679. https://doi.org/10.1016/j.meatsci.2005.09.017

Al-Murshedi, A. Y. M., Shabaa, G. J., Azooz, E. A., Naguib, I. A., Ul Haq, H., el Abbadi, N. K., & Snigur, D. (2025). Spectrophotometric determination of zinc in blood and food samples using an air-assisted rapid synergistic-cloud point extraction method based on deep eutectic solvents. *Journal of Food Composition and Analysis, 137*, Article 106910. https://doi.org/10.1016/j.jfca.2024.106910

Asaduzzaman, M., Ohya, M., Kumura, H., Hayakawa, T., & Wakamatsu, J. I. (2020). Searching for high ZnPP-forming edible bacteria to improve the color of fermented meat products without nitrite/nitrate. *Meat Science, 165*, Article 108109. https://doi.org/10.1016/j.meatsci.2020.108109

Benedini, R., Raja, V., & Parolari, G. (2008). Zinc-protoporphyrin IX promoting activity in pork muscle. *LWT- Food Science and Technology, 41*(7), 1160–1166. https://doi.org/10.1016/j.lwt.2007.08.005

Cavalheiro, C. P., Ruiz-Capillas, C., Herrero, A. M., & Pintado, T. (2021). Dry-fermented sausages inoculated with *enterococcus faecium* CECT 410 as free cells or in alginate beads. *LWT- Food Science and Technology, 139*, Article 110561. https://doi.org/10.1016/j.lwt.2020.110561

Chau, T. T., Ishigaki, M., Kataoka, T., & Taketani, S. (2010). Porcine ferrochelatase: The relationship between iron-removal reaction and the conversion of heme to Zn-protoporphyrin. *Bioscience Biotechnology and Biochemistry, 74*(7), 1415–1420. https://doi.org/10.1271/bbb.100078

Chen, Q., Hu, Y. Y., Wen, R. X., Wang, Y., Qin, L., & Kong, B. H. (2021). Characterisation of the flavour profile of dry fermented sausages with different NaCl substitutes using HS-SPME-GC-MS combined with electronic nose and electronic tongue. *Meat Science, 172*, Article 108338. https://doi.org/10.1016/j.meatsci.2020.108338

Dailey, H. A., Dailey, T. A., Wu, C. K., Medlock, A. E., Wang, K. F., Rose, J. P., & Wang, B. C. (2000). Ferrochelatase at the millennium: Structures, mechanisms and 2Fe-2S clusters. *Cellular and Molecular Life Sciences: CMLS, 57*(13–14), 1909–1926. https://doi.org/10.1007/pl00000672

Essid, I., & Hassouna, M. (2013). Effect of inoculation of selected *staphylococcus xylosus* and *lactobacillus plantarum* strains on biochemical, microbiological and textural characteristics of a tunisian dry fermented sausage. *Food Control, 32*(2), 707–714. https://doi.org/10.1016/j.foodcont.2013.02.003

Ghadiri Khozroughi, A., Kroh, L. W., Schluter, O., & Rawel, H. (2018). Assessment of the bacterial impact on the post-mortem formation of zinc protoporphyrin IX in pork meat. *Food Chemistry, 256*, 25–30. https://doi.org/10.1016/j.foodchem.2018.01.045

Gill, A. O., & Holley, R. A. (2003). Interactive inhibition of meat spoilage and pathogenic bacteria by lysozyme, nisin and EDTA in the presence of nitrite and sodium chloride at 24 °C. *International Journal of Food Microbiology, 80*(3), 251–259. https://doi.org/10.1016/s0168-1605(02)00171-x

Gøtterup, J., Olsen, K., Knøchel, S., Tjener, K., Stahnke, L. H., & Møller, J. K. S. (2008). Colour formation in fermented sausages by meat-associated *staphylococci* with different nitrite- and nitrate-reductase activities. *Meat Science, 78*(4), 492–501. https://doi.org/10.1016/j.meatsci.2007.07.023

Grossi, A. B., do Nascimento, E. S. P., Cardoso, D. R., & Skibsted, L. H. (2014). Proteolysis involvement in zinc-protoporphyrin IX formation during Parma ham maturation. *Food Research International, 56*, 252–259. https://doi.org/10.1016/j.foodres.2014.01.007

Gündoğdu, A. K., Karahan, A. G., & Çakmakç, M. L. (2006). Production of nitric oxide (NO) by lactic acid bacteria isolated from fermented products. *European Food Research and Technology, 223*(1), 35–38. https://doi.org/10.1007/s00217-005-0097-8

Guo, Q. W., Cui, B., Yuan, C., Guo, L., Li, Z., Chai, Q. Q., … Zhao, M. (2024). Fabrication of dry S/O/W microcapsule and its probiotic protection against different stresses. *Journal of the Science of Food and Agriculture, 104*(5), 2842–2850. https://doi.org/10.1002/jsfa.13175

Hayes, J. E., Canonico, I., & Allen, P. (2013). Effects of organic tomato pulp powder and nitrite level on the physicochemical, textural and sensory properties of pork luncheon roll. *Meat Science, 95*(3), 755–762. https://doi.org/10.1016/j.meatsci.2013.04.049

Hu, Y. Y., Li, Y. J., Zhu, J. M., Kong, B. H., Liu, Q., & Chen, Q. (2021). Improving the taste profile of reduced-salt dry sausage by inoculating different lactic acid bacteria. *Food Research International, 145*, Article 110391. https://doi.org/10.1016/j.foodres.2021.110391

Hu, Y. Y., Zhang, L., Zhang, H., Wang, Y., Chen, Q., & Kong, B. H. (2020). Physicochemical properties and flavour profile of fermented dry sausages with a reduction of sodium chloride. *LWT- Food Science and Technology, 124*, Article 109061. https://doi.org/10.1016/j.lwt.2020.109061

Jo, K., Lee, S., Yong, H. I., Choi, Y.-S., & Jung, S. (2020). Nitrite sources for cured meat products. *LWT- Food Science and Technology, 129*, Article 109583. https://doi.org/10.1016/j.lwt.2020.109583

Kauser-Ul-Alam, M., Hayakawa, T., Kumura, H., & Wakamatsu, J.-I. (2021). High ZnPP-forming food-grade lactic acid bacteria as a potential substitute for nitrite/nitrate to improve the color of meat products. *Meat Science, 176*, Article 108467. https://doi.org/10.1016/j.meatsci.2021.108467

Liu, C. J., Liu, Q., Jiang, B., Yan, J. F., & Qi, X. H. (2015). Antioxidative and cholesterol-rdducing ability of *Weissella viridescens* ORC4 from dry fermented sausages. *Journal of Food Science and Biotechnology, 34*(05), 512–516. https://doi.org/10.3969/j.issn.1673-1689.2015.05.011

de Maere, H., Fraeye, I., De Mey, E., Dewulf, L., Michiels, C., Paelinck, H., & Chollet, S. (2016). Formation of naturally occurring pigments during the production of nitrite-free dry fermented sausages. *Meat Science, 114*, 1–7. https://doi.org/10.1016/j.meatsci.2015.11.024

Mikami, N., Tsukada, Y., Pelpolage, S. W., Han, K.-H., Fukushima, M., & Shimada, K. (2020). Effects of sake lees (*sake-kasu*) supplementation on the quality characteristics of fermented dry sausages. *Heliyon, 6*(2), Article e03379. https://doi.org/10.1016/j.heliyon.2020.e03379

Morita, H., Niu, J., Sakata, R., & Nagata, Y. (1996). Red pigment of parma ham and bacterial influence on its formation. *Journal of Food Science, 61*(5), 1021–1023. https://doi.org/10.1111/j.1365-2621.1996.tb10924.x

Ning, C., Li, L., Fang, H. M., Ma, F., Tang, Y. X., & Zhou, C. L. (2019). L-lysine/L-arginine/L-cysteine synergistically improves the color of cured sausage with $NaNO_2$ by hindering myoglobin oxidation and promoting nitrosylmyoglobin formation. *Food Chemistry, 284*, 219–226. https://doi.org/10.1016/j.foodchem.2019.01.116

Parolari, G., Benedini, R., & Toscani, T. (2009). Color formation in nitrite-free dried hams as related to Zn-protoporphyrin IX and Zn-chelatase activity. *Journal of Food Science, 74*(6), C413–C418. https://doi.org/10.1111/j.1750-3841.2009.01193.x

Suman, S. P., & Joseph, P. (2013). Myoglobin chemistry and meat color. *Annual Review of Food Science and Technology, 4*, 79–99. https://doi.org/10.1146/annurev-food-030212-182623

Taketani, S., Ishigaki, M., Mizutani, A., Uebayashi, M., Numata, M., Ohgari, Y., & Kitajima, S. (2007). Heme synthase (ferrochelatase) catalyzes the removal of iron from heme and demetalation of metalloporphyrins. *Biochemistry, 46*(51), 15054–15061. https://doi.org/10.1021/bi701460x

Visessanguan, W., Benjakul, S., Smitinont, T., Kittikun, C., Thepkasikul, P., & Panya, A. (2006). Changes in microbiological, biochemical and physico-chemical properties of Nham inoculated with different inoculum levels of *lactobacillus curvatus*. *LWT- Food Science and Technology, 39*(7), 814–826. https://doi.org/10.1016/j.lwt.2005.05.006

Wakamatsu, J., Hayashi, N., Nishimura, T., & Hattori, A. (2010). Nitric oxide inhibits the formation of zinc protoporphyrin IX and protoporphyrin IX. *Meat Science, 84*(1), 125–128. https://doi.org/10.1016/j.meatsci.2009.08.036

Wakamatsu, J., Nishimura, T., & Hattori, A. (2004). A Zn-porphyrin complex contributes to bright red color in Parma ham. *Meat Science, 67*(1), 95–100. https://doi.org/10.1016/j.meatsci.2003.09.012

Wakamatsu, J., Okui, J., Ikeda, Y., Nishimura, T., & Hattori, A. (2004). Establishment of a model experiment system to elucidate the mechanism by which Zn-protoporphyrin IX is formed in nitrite-free dry-cured ham. *Meat Science, 68*(2), 313–317. https://doi.org/10.1016/j.meatsci.2004.03.014

Wakamatsu, J. I. (2022). Evidence of the mechanism underlying zinc protoporphyrin IX formation in nitrite/nitrate-free dry-cured Parma ham. *Meat Science, 192*, Article 108905. https://doi.org/10.1016/j.meatsci.2022.108905

Wakamatsu, J. I., Ito, T., Nishimura, T., & Hattori, A. (2007). Direct demonstration of the presence of zinc in the acetone-extractable red pigment from Parma ham. *Meat Science, 76*(2), 385–387. https://doi.org/10.1016/j.meatsci.2006.12.006

Wakamatsu, J. I., Okui, J., Hayashi, N., Nishimura, T., & Hattori, A. (2007). Zn protoporphyrin IX is formed not from heme but from protoporphyrin IX. *Meat Science, 77*(4), 580–586. https://doi.org/10.1016/j.meatsci.2007.05.008

Wannas, F. A., Azooz, E. A., Ridha, R. K., & Jawad, S. K. (2023). Separation and micro determination of zinc(II) and cadmium(II) in food samples using cloud point extraction method. *Iraqi Journal of Science, 64*(3), 1049–1061. https://doi.org/10.24996/ijs.2023.64.3.2

Wu, Y., Deng, J. L., Xu, F. R., Li, X., Kong, L. J., Li, C., & Xu, B. C. (2023). Zinc protoporphyrin IX generation by *Leuconostoc* strains isolated from bulged pasteurized vacuum sliced hams. *Food Research International, 174*, Article 113500. https://doi.org/10.1016/j.foodres.2023.113500

Yang, Q. H., Liu, Q., Chen, Q., Li, M., & Kong, B. H. (2023). Research progress on the formation and chromogenic mechanism of zinc protoporphyrin and its replacement for nitrite in meat products. *Food Science (in Chinese), 44*(23), 293–303. https://doi.org/10.7506/spkx1002-6630-20221220-196

Zajac, M., Zajac, K., & Dybas, J. (2022). The effect of nitric oxide synthase and arginine on the color of cooked meat. *Food Chemistry, 373*(Pt B), Article 131503. https://doi.org/10.1016/j.foodchem.2021.131503

Zhao, L., Jin, Y., Ma, C., Song, H., Li, H., Wang, Z., & Xiao, S. (2011). Physico-chemical characteristics and free fatty acid composition of dry fermented mutton sausages as affected by the use of various combinations of starter cultures and spices. *Meat Science, 88*(4), 761–766. https://doi.org/10.1016/j.meatsci.2011.03.010